



ELSEVIER

Journal of Magnetism and Magnetic Materials 164 (1996) 345–356



Relaxation of thermo-remanent magnetization in different magnetic phases of Fe-rich γ -FeNiCr alloys

G. Sinha^a, R. Chatterjee^{b,1}, M. Uehara^b, A.K. Majumdar^{a,*}

^a Department of Physics, Indian Institute of Technology, Kanpur 208 016, India

^b National Research Institute for Metals, 2-3-12, Nakameguro, Meguro-ku, Tokyo 153, Japan

Received 8 April 1996; revised 28 May 1996

Abstract

The time decay of the thermo-remanent magnetization (TRM) of the $\text{Fe}_{80-x}\text{Ni}_x\text{Cr}_{20}$ ($14 \leq x \leq 30$) alloys has been measured for four different magnetic phases within the fcc γ -phase using a SQUID magnetometer. In the spin-glass phase (SG) ($x = 19$) very distinct ageing effects are observed where $M(t)$ can be described as $M(t) = M_0(t/t_w)^{-\gamma} \exp[-(t/\tau)^{1-n}]$ for the entire time domain. In the re-entrant spin-glass (RSG) ($x = 23$ and 26), $M(t)$ can be better represented by the stretched exponential with an addition of a constant term which can be well explained by the Gabay–Toulouse (GT) model. We have also measured the linear and non-linear ac susceptibilities for the sample $x = 23$ and confirmed the presence of the ferromagnetic (FM) ordering down to the lowest temperature. In the RSG ($x = 23$), the TRM shows a minimum near T_c and a local maximum just above T_c . In the FM phase ($x = 30$), the popular prediction of the power law decay of the TRM is observed. The latter is indistinguishable from the stretched exponential in the antiferromagnetic (AF) phase ($x = 14$).

PACS: 75.30.Kz; 75.50.Bb; 75.50.Ee; 75.50.Lk

1. Introduction

Since the last decade, $\text{Fe}_{80-x}\text{Ni}_x\text{Cr}_{20}$ ($14 \leq x \leq 30$) alloys have been the subject of considerable interest because of their diverse magnetic properties within the same crystallographic phase [1]. These alloys exhibit a compositional phase transition from a long-range AF phase ($x = 14$) to a long-range FM one ($x = 30$), passing through intermediate phases of SG ($x = 19$) and RSG ($x = 23, 26$) with the increase of Ni concentration. The presence of the

strong competing ferro- [I(Ni–Ni), I(Fe–Ni), I(Ni–Cr), I(Fe–Cr)] and antiferromagnetic [I(Fe–Fe), I(Cr–Cr)] exchange interactions [2] is responsible for such rich magnetic phases. The complete phase diagram of these alloys was established by Majumdar and Blanckenhagen through dc magnetization and neutron diffraction measurements [1]. Later on ac susceptibility [3] and magnetoresistance measurements [4] also confirmed the proposed phase diagram. Taking advantage of the diverse magnetic properties of these alloys *within the same fcc γ -phase*, we tried to understand the age-old problem of relaxation dynamics. This area has always been in the front-line because of its multiple complexities and wide varieties. In this paper, we present the dynam-

* Corresponding author. Email: akm@iitk.ernet.in.

¹ Permanent address: Department of Physics, Indian Institute of Technology, New Delhi 110 016, India.

ics of time and temperature-dependent magnetic relaxations in various magnetic phases.

The search for magnetic relaxation began a century back, when Ewing [5] observed persistence of magnetization in soft iron for significant amount of time and a non-exponential decay. Richter [6] observed logarithmic decay of magnetization for about one decade of time in carbonised iron. Street and Woolley [7] and Néel [8] also predicted a logarithmic decay of TRM in FMs. Several theoretical and experimental evidences suggest that an anomalous slower relaxation of the form

$$M(t) = M_0 \exp\left[-(t/\tau)^\beta\right], \quad 0 < \beta < 1, \quad (1)$$

is far more reasonable and common than the conventional Debye exponential form ($\beta = 1$). In fact, this kind of relaxation has been observed for a wide range of phenomena and materials [9]. In 1970, Williams and Watts [10] postulated similar functions for dielectric relaxation ($\beta = 0.5$). In a review article Jonscher [11] summarized the experimental evidence on the frequency, time, and temperature dependence of the dielectric response for a wide range of solids. He also found a universality of dielectric behaviour and proposed a generalized approach of many-body interaction. The structural relaxation rate, in the case of liquid to glass transition, can be expressed as a stretched exponential ($\frac{2}{3} < \beta < 1$) [12]. Also the validity of this functional form for the relaxation of TRM in SG's has been reported by a large number of investigators [13–17]. Palmar et al. [18] presented in an elegant fashion the whole scenario of similar kinds of relaxation in complex, slowly relaxing, and strongly interacting materials. They considered series relaxation and hierarchically constrained dynamics which is distinctly different from other approaches [19] of getting similar results. Hammann et al. proposed a phenomenological picture of the dynamic properties of SG's based on fractal cluster model [20,21]. Early decay measurements of TRM of spin glasses had shown logarithmic dependence [22]. Similar dependence was also observed in AuFe, AgMn, and ThGd spin-glasses from 5 to 10^4 s [23]. Analysing the neutron diffraction and ac susceptibility data, Murani [24] found power law decay for shorter time and logarithmic decay for longer time below T_g in SG's. Bontemps and Orbach [25] mea-

sured the TRM of the insulating SG $\text{Eu}_{0.4}\text{Sr}_{0.6}\text{S}$ between $0.86T_g$ and $1.04T_g$. They found power law decay of the TRM for shorter interval of time and a stretched exponential decay beyond a well-defined cross-over time.

Recently two different theoretical models have been proposed to describe the SG behaviour. The first is the mean-field approach of Parisi's solution [26] of infinite range Sherrington–Kirkpatrick (S–K) [27] model by considering hierarchical organizations of infinite number of quasi-equilibrium states in phase space [28]. The second is the phenomenological approach based on the existence of a distribution of droplets [29] or dynamical domains [30] of correlated spins. Both these theories can explain reasonably well the slower SG dynamics and ageing effects. A nice comparison between these two models was given by Lefloch et al. [31]. Huse and Fisher [29] proposed long time decay as stretched exponential with exponent $1/2$ by using droplet fluctuations in two dimensional pure Ising system with a spontaneously broken continuous symmetry. In the framework of droplet fluctuations [29], the spin autocorrelation can be described as exponentially rare in $\ln t$: $c_i(t) = \exp[-k(\ln t)^y]$ (where $y = 1$ for random exchanges, $y = d - 2/d - 1$ for random fields) in random FM's and power of $\ln t$ in SGs. Ogielski [32] predicted that the spin autocorrelation function can be described by the product of power law and stretched exponential at all temperatures above T_g [33] and by power law below T_g . Ocio et al. found an analytical expression based on scaling analysis of ageing effects, for the decay of TRM in the SG, CsNiFeF_6 [34] as well as in AgMn [35]. They proposed the decay of TRM as

$$M(t) = M_0(\lambda)^{-\alpha} \exp\left[-(\omega\lambda/t_w^\mu)^{1-n}\right], \quad (2)$$

with

$$\lambda = (t_w/(1 - \mu)) \left[(1 + t/t_w)^{1-\mu} - 1 \right], \quad (3)$$

where λ is the effective time and μ is an exponent smaller than 1. A different analysis, based on the S–K mean-field model [36], suggests algebraic decay. In ferromagnets attempts have been made to explain the magnetic relaxation using a model based on magnon relaxation on a percolation distribution of

finite domains [37]. The other popular prediction of relaxation is the power law [38] decay which can be obtained from scaling theories for domain growth [39] and internal dynamics [40]. Ikeda and Kikuta [41] found that there is no magnetic relaxation over 10 h in the AF, $\text{Mn}_{0.45}\text{Zn}_{0.55}\text{F}_2$ at slightly lower temperatures than the transition temperature.

Despite considerable experimental work on relaxation dynamics covering enormous range of time window, no conclusive results have been found. Moreover, there is a lack of clear distinction between the SG and the RSG phases. Also no experimental data are available on relaxation dynamics in the AF phase. All these have motivated us to study systematically the relaxation dynamics in four different magnetic phases, namely, SG, RSG, FM and AF in FeNiCr alloys *within the same crystallographic phase*, for different wait times and at different temperatures for the largest available time window. There is a running controversy about the existence of FM ordering in RSG at the lowest temperature as predicted by the GT model [42]. We have also measured linear and non-linear ac susceptibilities for the sample $x = 23$ to resolve this controversy.

2. Experimental procedure

All these ternary alloys were prepared by induction melting in argon atmosphere. The starting materials were of 99.999% purity obtained from M/s Johnson Matthey Inc., England. The alloys were cut to the required size, homogenized at 1323 K for 100 h in an argon atmosphere, and then quenched in oil.

Chemical analysis of Ni and Cr shows that the compositions of the alloys are within ± 0.5 at% of their nominal values. X-ray diffraction data at room temperature in powdered samples reveal that these are single-phase fcc (γ) alloys with the lattice parameter $a = 3.60$ Å. Neutron diffraction data show the presence of single-phase fcc (γ) structure down to 2 K for $x = 14$ and 19.

The two most essential ingredients of a SG are frustration and quenched disorder which manifest themselves in history-dependent phenomena and eventually lead to a nonequilibrium behaviour below T_g [43]. To study the relaxation dynamics, we applied a small magnetic field (10 gauss) at a tempera-

ture greater than the characteristic temperatures (T_g , T_c , T_N), cool (t_c = cooling time) the system to a temperature T_m which is less than the characteristic temperature. This field-cooled system will attain a metastable state (which is not an equilibrium state) [14,44], then after waiting for definite amounts of time t_w (t_w varies from 60 to 3600 s) the magnetic field is removed, the system is allowed to relax towards the equilibrium state and then the TRM is measured with time (30 to 12000 s) using a SQUID magnetometer (Quantum Design MPMS). To see the effect of temperature, we also measured TRM at several temperatures, T_m , both above and below the characteristic temperatures for constant wait time, $t_w = 180$ s. We have very carefully subtracted the background noise. We repeated the experiments and obtained similar results within the experimental error.

3. Results and discussion

The most salient feature of the present work is to demonstrate how by changing the composition by small amounts in $\text{Fe}_{80-x}\text{Ni}_x\text{Cr}_{20}$ alloys ($x = 14$ AF, $x = 19$ SG, $x = 23, 26$ RSG, $x = 30$ FM) one can tune the relaxation dynamics. This is the only experimental report which presents a complete scenario of the relaxation spectrum in various kinds of interesting magnetic phases and throws new light on this area of interest to theoreticians as well as experimentalists.

3.1. Spin glass ($x = 19$)

We observe remarkable results of ageing effects in the SG where each isotherm strongly depends upon wait time t_w (time of exposure in magnetic field below T_g). The magnetization can be well represented by an equation of the form

$$M(t) = M_0(t/t_w)^{-\gamma} \exp\left[-(t/\tau)^{1-n}\right] \quad (4)$$

for the entire available time domain. Fig. 1 shows the time decay of TRM, $M(t)$, for different wait times ($t_w = 60, 240, 1200, 1800, 3600$ s) below T_g (12 K) at $T_m = 5$ K for the SG ($x = 19$) and the solid lines are the best fits of the experimental data

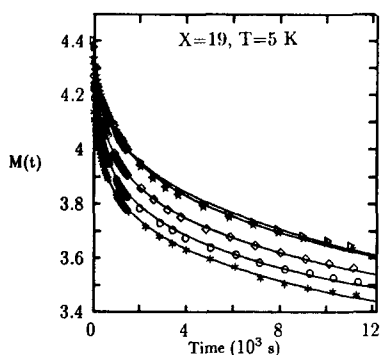


Fig. 1. TRM, $M(t)$ (10^{-2} emu/g), as a function of time in the SG ($x = 19$) at 5 K for $t_w = 3600, 1800, 1200, 240$ and 60 s, from top to bottom, respectively. Solid lines are the best fits of the data to Eq. (4).

to Eq. (4) ($\chi^2 = (1/n) \sum_{i=1}^n (\text{Raw data}_i - \text{Fitted data}_i)^2 / \text{Raw data}_i^2 \leq 10^{-6}$). We have purposefully plotted our data on a linear time scale because if we plot on a log scale, for longer time interval, the plot will contract and the fits will apparently look better. However, goodness of fit is better judged from the value of χ^2 . From these fits, the value of the initial TRM, M_0 , the characteristic time constant, τ , and the exponents, n and γ , are found. The most significant feature of this analysis is that M_0 (≈ 0.04 emu/g) is not varying with t_w [44,14,35] while the exponent, n , gradually increases with the increase of t_w . This indicates that larger time exposure below T_g in a magnetic field makes the system more reluctant to come back to an equilibrium state from a metastable one. Other investigators [44,14] reported n independent of wait time but we found that it varies from 0.63 to 0.77. The power law exponent, γ , remains constant (0.022 ± 0.004) except $t_w = 60$ s where γ is 0.03.

Fig. 2 shows the variation of TRM, $M(t)$, with time for different temperatures at a constant wait time ($t_w = 180$ s). From the best fit to Eq. (4) the temperature variations of n , M_0 , τ , and γ are found which broadly match with the previous observations [44,14,35,45]. The value of n increases linearly from 0.8 to 0.9 from $0.5T_g$ to T_g and then it starts falling beyond T_g (Fig. 3). It is reported that in the SG AgMn and CuMn, n remains constant at lower temperatures and then it starts rising from a temperature $T = T_0$, which strongly depends on the anisotropy energy of the sample [48] and hence can vary from

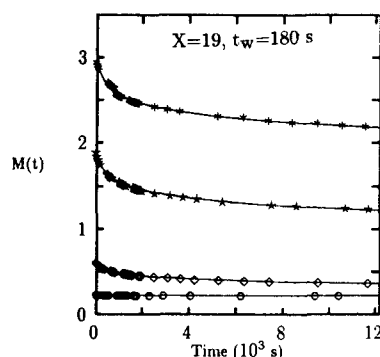


Fig. 2. TRM, $M(t)$ (10^{-2} emu/g), as a function of time in the SG ($x = 19$) for $t_w = 180$ s for different temperatures, $T_m = 7, 9, 12$ and 15 K, from top to bottom, respectively. Solid lines are the best fits of the data to Eq. (4).

sample to sample. Non-availability of lower temperature data (less than $0.4T_g$) prevented us from verifying the constancy of n . The prefactor, M_0 , shows (Fig. 3) a linear decrease with increasing temperature for $T < 0.75T_g$ and the rate of decrease becomes slower for $T > 0.75T_g$, in good agreement with the earlier findings [44]. The power law exponent γ increases with the increase of temperature up to $0.75T_g$. At T_g and beyond it starts decreasing with temperature (Fig. 3). It is difficult to tell exactly the temperature from which it has started falling, but the earlier prediction was that it should increase as one approaches T_g [35]. Fig. 4 shows how the inverse of the characteristic relaxation time τ decreases with the increase of the reduced temperature T_g/T for $x = 19$. This was also observed by Alba et al. [35] in

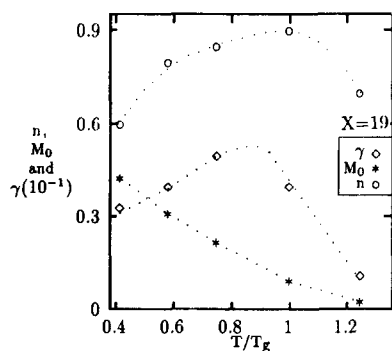


Fig. 3. Temperature variation of the exponents, γ and n , and the initial magnetization, M_0 (10^{-1} emu/g), for $t_w = 180$ s in the SG ($x = 19$). Dotted lines are just guides to the eye.

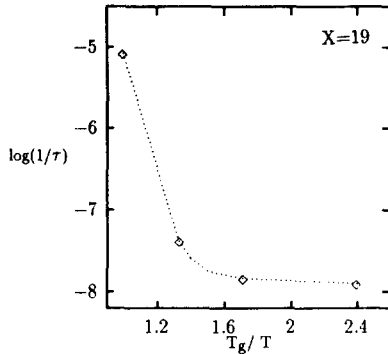


Fig. 4. Temperature variation of the inverse of the characteristic relaxation time, $1/\tau$, (semi-log) for $t_w = 180$ s in the SG ($x = 19$). Dotted line is just a guide to the eye.

AgMn. Fig. 4 also reflects the general tendency observed by others [14,46]. Fewer number of data points prevents us from finding the functional form. Apparently, to check the exponential form as predicted earlier [14], we need to probe even at lower temperatures. We can try to explain the variation of τ with temperature by considering hierarchically organized metastable states in phase space [31] within the framework of Parisi's mean-field solution of the infinite range S–K model. The states are continuously splitting into new states with the lowering of temperature and are separated by barriers. These barrier heights strongly vary inversely with temperature. That is, at lower temperatures, barrier heights increase and separate different metastable states into mutually inaccessible states which makes τ larger at lower temperatures. Using values of n and τ from Figs. 3 and 4, respectively and plotting $\log(1 - n)(1/\tau)^{1-n}$ versus $(1 - n)$ by writing this function as $(1 - n)(1/\tau)^{1-n} = c\omega^{1-n}$, we get the value of the relaxation frequency ω from the slope of the best-fitted curve (Fig. 5) as $1.9 \times 10^{-7} \text{ s}^{-1}$ and the constant, c , is 0.13. These values are much slower than those predicted earlier [13]. Analysis of $M(t)$ by considering only the stretched exponential, i.e., without the power law part of Eq. (4), shows unusually small (≈ 10 times smaller) values of n and a poor $\chi^2 (\approx 10^{-5})$. Fits are even poorer in cases of other mathematical forms, like the power law. So, we find that Eq. (4) is the simplest analytical form that can represent our experimental data of the decay

of TRM in the SG phase for the available time domain.

We should mention here that Eq. (4) is a simpler version of the earlier prediction of scaling analysis of ageing process [35,34] (Eq. (2)). Instead of t they used λ which is a function of t and t_w and $\lambda \rightarrow t$ for $t < t_w$. But we find that Eq. (4) is valid for the entire available time domain. FeNiCr alloys show some unconventional behaviour in different magnetic phases. From our magnetoresistance (MR) measurements [4] we concluded that these alloys do not show distinctive features of any pure magnetic phase. This could be understood in terms of very strong competing antiferro (Fe–Fe, Cr–Cr) and ferromagnetic (all other pairs) interactions which prevent the formation of well-defined pure magnetic phases. Hence the direct comparison of Eq. (2) with our result is difficult. Ogielski [32] predicted similar analytical form to describe the spin autocorrelation function in SG at all temperatures above T_g for both short and long time scales. However other investigators [13,16,45] found only the stretched exponential form for the decay of TRM for the SG phase.

Chu et al. [46] in a recent paper, reported that for longer wait times remanence should be large and the decay of TRM becomes slower as we had observed. They also calculated the field dependence of the exponent (n) which does not vary significantly from 4 to 30 gauss. For fields > 50 gauss, n increases significantly. We have repeated some of our experiments in 20 gauss field and could not observe any change in the exponents.

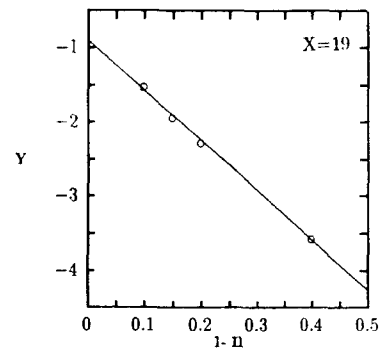


Fig. 5. $Y = \log((1 - n)(1/\tau)^{1-n}) = \log(c\omega^{1-n})$ as a function of $(1 - n)$ for different temperatures for $t_w = 180$ s in the SG ($x = 19$). Solid line is the best fit for getting ω .

3.2. Re-entrant spin glass ($x = 23$ and 26)

The SG has been the focus of attention for quite sometime, but not much attention has been paid to the RSG phase. The sample with $x = 23$, below 35 K, enters a FM phase from a random paramagnetic (PM) phase. On further lowering of temperature below 22 K it enters once again a new random phase where FM and SG orderings coexist [1]. It shows most of the SG-like behaviour (frustration, irreversibility, etc.). This phase is known as the RSG.

We observe in the RSG that the best representation of TRM is

$$M(t) = M_1 + M_0 \exp\left[-(t/\tau)^{1-n}\right]. \quad (5)$$

The additional small term M_1 can easily be explained in the framework of the GT model [42] where only transverse spin freezing occurs in the RSG while the longitudinal spins can produce diffuse background effect.

Fig. 6 represents the variation of $M(t)$ with time at $T_m = 5$ K for different wait times ($t_w = 60, 1200, 1800$, and 3600 s) in the RSG phase ($x = 23$) and the solid lines are the best fitted curves which are of the form of Eq. (5) ($\chi^2 \approx 10^{-6} - 10^{-7}$). The salient feature of this figure is that the initial magnetization, $\sigma_0 = M_0 + M_1$, increases with the increase of wait time (Fig. 7). This is not observed in the SG phase but the variation of n is similar. We also observe that M_1 , which is arising because of the presence of the FM ordering [42], is not changing at all with wait

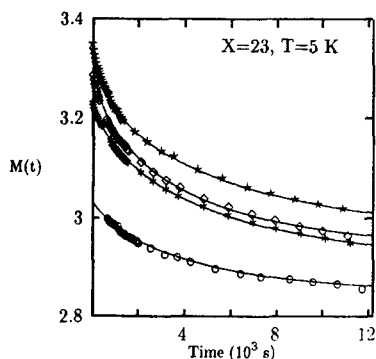


Fig. 6. TRM, $M(t)$ (10^{-1} emu/g), as a function of time in the RSG ($x = 23$) at 5 K for $t_w = 3600, 1800, 1200$ and 60 s, from top to bottom, respectively. Solid lines are the best fits of the data to Eq. (5).

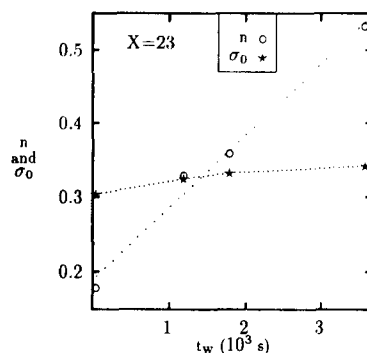


Fig. 7. Wait time dependence of the exponent, n , and the initial magnetization, σ_0 (emu/g), at 5 K in the RSG ($x = 23$). Dotted lines are just guides to the eye.

time and the values of M_1 are 84 to 94% of the total magnetization depending on wait time (total magnetization changing with wait time). It is quite natural that if the ferromagnetic component is embedded in the SG phase, then the major contribution of the total magnetization should come from the ferromagnetic component. A similar expression (Eq. (5)) was also reported earlier for the decay of TRM in SG's as well as in RSG's [47]. But they did not find any difference between the RSG and the SG phases. We find that Eq. (5) is only valid for the RSG and distinct differences exist between the SG and the RSG phases.

Fig. 8 depicts the variation of $M(t)$ with time at different temperatures ($T_m = 10, 15, 20, 25, 30$, and 38 K) for constant wait time (180 s). From the fits of the data to Eq. (5), the value of σ_0 and the exponent, n , are found. The exponent increases with temperature and approaches unity as one approaches T_g , in exact agreement with the previous observations [13,14] in SG's, the only difference is that the present values are slightly higher. If we increase the temperature even more, a sudden change takes place around 20 K. A drop in the value of n indicates a phase change. Moreover, at lower temperatures it shows a better fit to Eq. (5) but at higher temperatures power law fit is better than the stretched exponential. This supports the on-set of the FM phase. This could also be an indication of the switch-over from nonequilibrium dynamics to equilibrium dynamics when it passes from the RSG to the FM phase. The power law behaviour in the FM phase

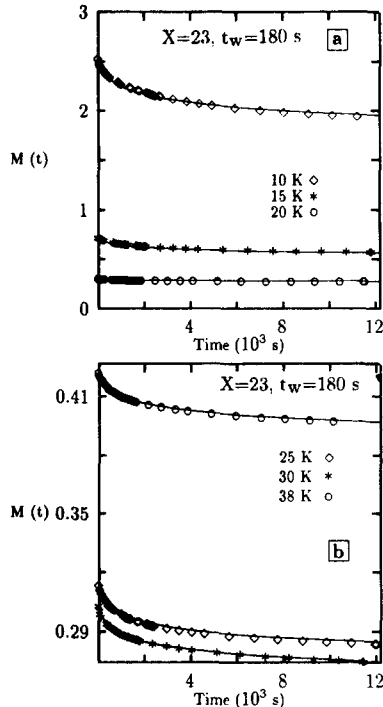


Fig. 8. TRM, $M(t)$ (10^{-1} emu/g), as a function of time in the RSG ($x=23$) for $t_w=180$ s for different temperatures. (a) $T_m=10, 15$ and 20 K, and (b) $38, 25$ and 30 K, from top to bottom, respectively. Solid lines are the best fits of the data to Eq. (5).

(having an exponent ≈ 0.06) is quite consistent with the Huse and Fisher theory [29]. The rate of increase of the exponent also changes somewhat beyond 30 K where it passes from the FM to the PM state at 35 K. The value of the exponent varies by 4.6% in the temperature interval of 8 K (30 to 38 K) (Fig. 9). This is above the error bar which is less than 1% . The size of the symbol (Fig. 9) is of the order of the error bar. The value of the exponent shows anomaly near two temperatures, 22 K and 35 K, which are nothing but T_g and T_c , respectively [1]. But the variation of n near T_c is not as prominent as that near T_g . We also find that in Eq. (5) the additional term, M_1 , which is the value of the residual magnetization, $M(\infty)$, decreases with the increase of temperature below T_g (0.0067 emu/g at T_g) and suddenly increases to 0.027 emu/g when it enters the FM phase, as expected. The most striking observation is the variation of the initial magnetization, σ_0 , with temperature (Fig. 9). σ_0 decreases monotonically

with the increase of temperature up to 20 K beyond which the rate of decrease reduces significantly and at 25 and 30 K it becomes almost constant (0.033 and 0.032 emu/g, respectively) and then there is a sudden rise at 38 K (0.045 emu/g) which makes the scenario most interesting. The value of σ_0 changes by about 40% in this temperature interval (30 to 38 K). This kind of remarkable observation of switching of magnetization while passing from FM to PM phase was reported earlier only by Chamberlin and Holtzberg [48] in ferromagnetic EuS single crystal. They tried to explain this in terms of the percolation theory [49]. So we observe that the TRM in the RSG ($x=23$) shows a minimum near T_c and a local maximum just beyond T_c . At lower temperatures ($< T_c$), the finite size domains try to orient themselves with the direction of the local field, which need not be in the same direction as the applied field. These domains are dynamically strongly correlated (forming a strong viscous medium). FeNiCr alloys have shown very large high-field susceptibility [50], i.e., even at very high magnetic fields the orientation of these domains with the direction of the applied field is not complete because of the presence of strong anisotropy. Near T_c the correlation between finite domains gets disrupted. Just above T_c , the domain magnetization still remains but the domains become less viscous and they try to orient themselves along the direction of the applied field, thus increasing the magnetization. Further increase of temperature randomizes the whole spin orientation. We repeated the experiment to confirm this unusual observation and found similar behaviour.

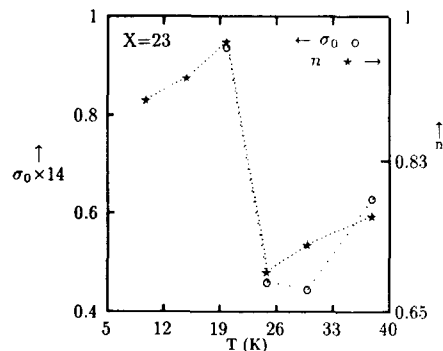


Fig. 9. Temperature variation of the exponent, n , and the initial magnetization, σ_0 (emu/g), for $t_w=180$ s in the RSG ($x=23$). Dotted lines are just guides to the eye.

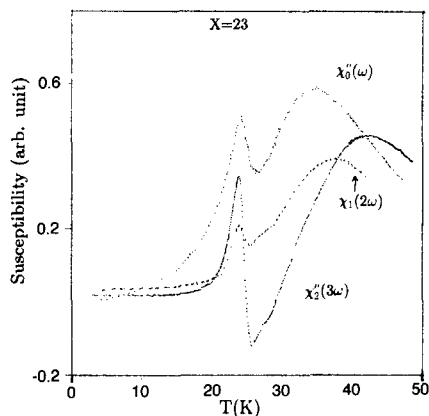


Fig. 10. Temperature variation of the linear (χ_0'') and non-linear (χ_1' , χ_2'') ac susceptibilities in the RSG ($x=23$) (ac field = 0.6 gauss and frequency $\omega = 242$ Hz). We multiply the raw data by different appropriate scaling factors to bring them in one graph.

In general the non-linear magnetization in the presence of a magnetic field (h), can be written as $m = m_0 + \chi_0 h + \chi_1 h^2 + \chi_2 h^3 + \dots$, where m_0 = spontaneous magnetisation, χ_0 linear- and χ_1 , χ_2 , etc., are nonlinear susceptibilities, and $h = h_0 \sin \omega t$ for ac field. In SG where no spontaneous magnetization exists, only odd harmonics of the susceptibility will be present [51,52]. We observe that the out-of-phase part of the linear ac susceptibility (χ_0'') shows peaks [52] near T_g and T_c , respectively (Fig. 10) (ac field of 0.6 Oe and frequency $\omega = 242$ Hz). Similar peaks are observed in χ_2'' ($\partial^3 m / \partial h^3$, out-of-phase part of the third harmonics). The distinct peak near T_g for $x=23$ is consistent with the theoretical predictions [52,53]. χ_1' ($\partial^2 m / \partial h^2$, second harmonics) also shows a distinct peak near T_g (Fig. 10) which is never observed in a pure SG, including $x=19$. This indicates the presence of a ferromagnetic component in the RSG down to the lowest temperature. So, we find that the RSG shows the SG transition and also the presence of FM ordering below T_g . This distinguishes it from the SG. Detailed studies of ac susceptibilities in FeNiCr alloys will be published elsewhere [54].

The sample with $x=26$, below 56 K, enters a FM phase from a random PM phase. On further lowering of temperature below 7 K it enters an RSG phase [1]. We observe some different features in the samples $x=23$ and $x=26$, though they undergo similar kinds of phase transitions (PM \rightarrow FM \rightarrow

RSG). $M(t)$ data at 5 K, similar to those shown in Fig. 6 but now for the sample $x=26$, when fitted to Eq. (5) ($\chi^2 \approx 10^{-6} - 10^{-7}$), shows that the initial magnetization, $\sigma_0 = M_0 + M_1$, does not change with wait time (≈ 0.5 emu/g). The value of the exponent, n , increases from 0.55 to 0.64, with the increase of wait time from 240 to 3780 s. We have observed similar variation in the SG ($x=19$) phase whereas in the other sample, $x=23$, σ_0 increases with wait time in the RSG phase. The value of σ_0 is larger for the sample $x=26$ than that for the sample $x=23$ and smaller than that for the sample $x=30$ (FM, described below). Hence the value of the initial magnetization, σ_0 , increases gradually with the increase of Ni concentration as we move towards the FM phase. The variation of n is similar in both the SG ($x=19$) and the RSG ($x=23$) samples. Fig. 11 displays the variation of $M(t)$ with time at different temperatures ($T_m = 6, 8, 10, 20, 30, 40, 50$, and 60 K) for constant wait time (180 s) for the sample

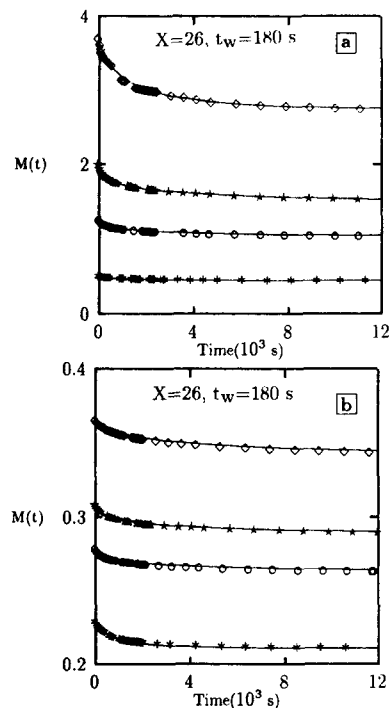


Fig. 11. TRM, $M(t)$ (10^{-1} emu/g), as a function of time in the RSG ($x=26$) for $t_w=180$ s for different temperatures. (a) $T_m = 6, 8, 10$, and 20 K, and (b) 30, 40, 50, and 60 K, from top to bottom, respectively. Solid lines are the best fits of the data to Eq. (5).

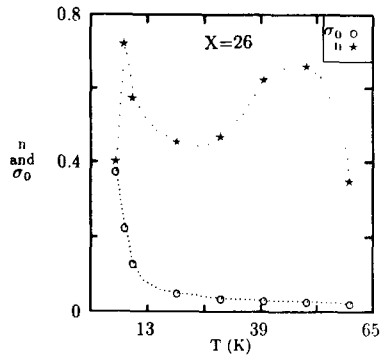


Fig. 12. Temperature variation of the exponent, n , and the initial magnetization, σ_0 (emu/g), for $t_w = 180$ s in the RSG ($x = 26$). Dotted lines are just guides to the eye.

$x = 26$. From the fits ($\chi^2 \approx 10^{-6} - 10^{-7}$) of the data to Eq. (5), the values of initial magnetization, σ_0 , and the exponent, n , are found. σ_0 decreases at a faster rate up to 20 K and then continues to decrease slowly till 60 K (Fig. 12). Here we have not observed the local maximum above T_c as in the case of $x = 23$. To observe this we need to probe at a temperature closer to T_c (56 K). The exponent, n , increases abruptly when the system undergoes a transition from the RSG to the FM phase at 7 K. Then it starts to decrease up to 20 K and beyond this again increases till 50 K. Further increase of temperature reduces the value of n and the system passes from the FM to the PM phase (Fig. 12). The variation of n is not well understood, specially the dip around 20 K. Interestingly, we have also observed

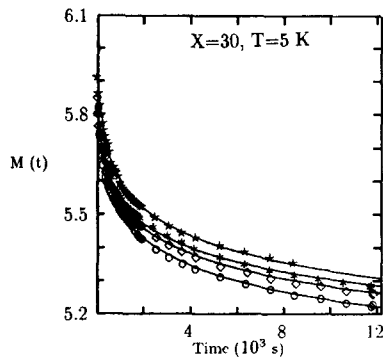


Fig. 13. TRM, $M(t)$ (10^{-1} emu/g), as a function of time in the FM ($x = 30$) at 5 K for $t_w = 3780, 1980, 1380$ and 240 s, from top to bottom, respectively. Solid lines are the best fits of the data to the power law (Eq. (6)).

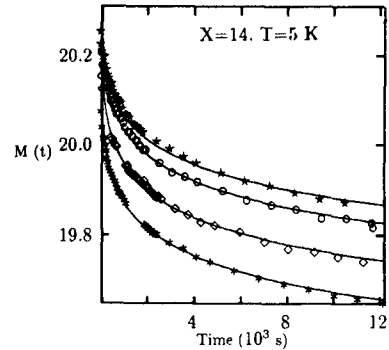


Fig. 14. TRM, $M(t)$ (10^{-4} emu/g), as a function of time in the AF ($x = 14$) at 5 K for $t_w = 3780, 1980, 1320$ and 180 s, from top to bottom, respectively. Solid lines are the best fits of the data to the power law (Eq. (7)).

around this temperature some striking features in the low-field magnetoresistance and ac susceptibility measurements [54]. These features have kept the field wide open for further work. We also observe that at higher temperatures ($T \geq 30$ K, much higher than T_g) $M(t)$ data show better fits to the power law compared to the stretched exponential (Eq. (5)). For $x = 23$, we observe similar behaviour for $T \geq T_g$.

3.3. Ferromagnet ($x = 30$) and antiferromagnet ($x = 14$)

Fig. 13 shows the variation of TRM with time at 5 K in the FM phase ($x = 30$) for different wait times ($t_w = 240, 1380, 1980, 3780$ s). We find that $M(t) = M_1 + M_0 t^{-\gamma}$

(6)

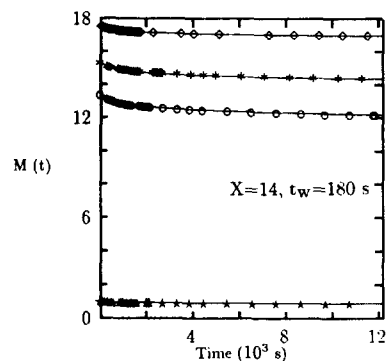


Fig. 15. TRM, $M(t)$ (10^{-4} emu/g), as a function of time in the AF ($x = 14$) for $t_w = 180$ s for different temperatures, $T_m = 10, 18, 24$ and 30 K, from top to bottom, respectively. Solid lines are the best fits of the data to the power law (Eq. (7)).

Table 1

Best fitted parameters for the power law (Eq. (7)) for different wait times at 5 K for $x = 14$. Solid lines in Fig. 14 are the best fitted curves. χ^2 is defined in the text

t_w (10^3 s)	M_0 (10^{-4} emu/g)	γ (10^{-4})	χ^2 (10^{-7})
0.18	20.58	44.0	0.59
1.32	20.57	43.5	1.03
1.98	20.62	41.6	2.22
3.78	20.61	38.2	3.30

gives the best fit of the experimental data (solid lines in the graph) and from the fits ($\chi^2 \approx 10^{-6} - 10^{-7}$) the values of M_1 , M_0 and γ are found. It does not show much wait-time dependence, the values of M_1 and M_0 remain almost constant (≈ 0.29 and 0.35 ± 0.01 emu/g, respectively) while the exponent, γ , decreases inversely with wait time (from 0.049 to 0.036). With the increase of temperature the value of the initial magnetization reduces drastically (0.65 emu/g at 5 K to 0.094 emu/g at 80 K) and the exponent also becomes smaller (0.049 at 5 K to 0.00036 at 80 K).

Fig. 14 shows the time decay of TRM, $M(t)$, for different wait times ($t_w = 180, 1320, 1980, 3780$ s) below $T_N = 26$ K ($T_m = 5$ K) for the AF ($x = 14$) sample and the solid lines are the power law fits of the form

$$M(t) = M_0 t^{-\gamma}. \quad (7)$$

From these fits the values of M_0 and γ are obtained (Table 1). M_0 (≈ 0.00206 emu/g) does not change with wait time whereas γ decreases with the increase of wait time (0.0044 to 0.0038). Fig. 15 shows the time decay of TRM, $M(t)$, at different temperatures for constant wait time (180 s) and the solid lines are the power law fits from which the

Table 2

Best fitted parameters for Eq. (1) for different wait times at 5 K for $x = 14$

t_w (10^3 s)	M_0 (10^{-4} emu/g)	β (10^{-4})	χ^2 (10^{-7})
0.18	53.9	43.8	0.63
1.32	54.0	43.6	2.62
1.98	54.1	43.4	1.09
3.78	54.2	39.7	3.40

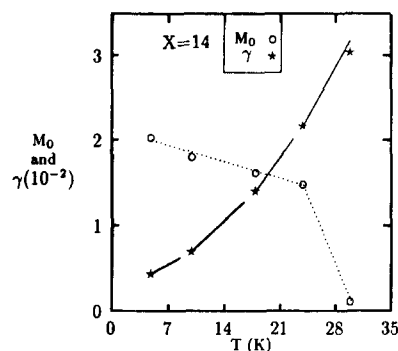


Fig. 16. Temperature variation of the exponent, γ , and the initial magnetization, M_0 (10^{-3} emu/g), for $t_w = 180$ s in the AF ($x = 14$). Dotted lines are just guides to the eye.

value of M_0 and γ are found (Table 3). The value of M_0 decreases linearly with the increase of temperature up to T_N (0.0015 emu/g at 24 K) and then suddenly falls to a much lower value (0.00012 emu/g at 30 K) as shown in Fig. 16. The exponent, γ , increases with temperature and the rate of increase changes somewhat when it passes to the PM phase (Fig. 16). In case of the AF phase we need not add any constant term (unlike the FM phase) and the value of the exponent is an order of magnitude lower than that in the FM phase. We also observe that the stretched exponential function, Eq. (1), shows reasonably good fits to the TRM in the AF phase. The value of the best-fitted parameters and the χ^2 are given in Tables 2 and 4. The value of the exponent, β , is almost two orders of magnitude smaller than that in the SG phase (0.004 and 0.37, respectively). It increases monotonically (Table 4) with temperature (0.004 at 5 K to 0.029 at 30 K) in contrast to that in the SG phase where β decreases with the

Table 3

Best fitted parameters for the power law (Eq. (7)) at different temperatures for constant wait time (180 s) for $x = 14$. Solid lines in Fig. 15 are the best fitted curves

T (K)	M_0 (10^{-4} emu/g)	γ (10^{-3})	χ^2 (10^{-7})
5	20.5	4.0	0.59
10	18.2	7.0	0.63
18	16.3	14.0	3.39
24	14.9	21.7	3.90
30	1.2	30.4	34.0

Table 4

Best fitted parameters for Eq. (1) at different temperatures for constant wait time (180 s) for $x = 14$

T (K)	M_0 (10^{-4} emu/g)	β (10^{-3})	χ^2 (10^{-7})
5	53.9	4.4	0.63
10	47.1	7.0	0.71
18	40.0	14.0	2.50
24	35.0	19.0	79.0
30	2.4	29.0	27.0

increase of temperature up to T_g (0.37 at 5 K to 0.1 at 12 K obtained from Fig. 3 using $\beta = 1 - n$). So, we find that the $M(t)$ data for the AF fit well to both the power law (Eq. (7)) and the stretched exponential (Eq. (1)). We have given the values of χ^2 in Tables 1–4 for comparison. They are comparable for both the above mathematical forms. Hence it is difficult to describe the exact nature of the decay of the TRM in the AF phase. More experimental work is needed to arrive at a more definite conclusion.

4. Conclusions

We have measured the TRM in $\text{Fe}_{80-x}\text{Ni}_x\text{Cr}_{20}$ ($14 \leq x \leq 30$) alloys for four different magnetic phases within the *same crystallographic phase* and from their wait time and temperature variations tried to establish a correspondence with the phase diagram. We find distinct differences between the SG and the RSG phases with two different analytical forms for the time decay of the TRM. We also observe the presence of the FM ordering in the RSG below T_g which is consistent with the GT model. The peak in χ_1 near T_g for RSG ($x = 23$) had never been observed in any pure SG, including $x = 19$. The peak can only be observed if spontaneous magnetization is present. Hence we confirm the presence of the FM ordering in the RSG down to the lowest temperature. This feature distinguishes the RSG from the SG. We also report the remarkable observation of the local maximum of the TRM just above T_c in the RSG ($x = 23$) when it passes to the PM phase from the FM phase. This is found for the first time in any polycrystalline RSG. However, its exact theoretical justification is unclear. We also observe that the

values of the exponents show anomaly near the phase transitions. We observe some different features in the samples $x = 23$ and $x = 26$, though they undergo similar kinds of phase transitions. We find the conventional power law decay in the FM phase. The value of the magnetization is found to increase with the Ni concentration. In the AF phase the power law decay is indistinguishable from the stretched exponential as a description of the TRM. More experimental work is needed to arrive at a more definite conclusion about the decay of TRM in AF.

Acknowledgements

Financial assistance from project No. SP/S2/M-45/89 of the Department of Science and Technology, Government of India, is gratefully acknowledged.

References

- [1] A.K. Majumdar and P. v. Blanckenhagen, Phys. Rev. B 29 (1984) 4079; J. Magn. Magn. Mater. 40 (1983) 227.
- [2] A.Z. Men'shikov, N.N. Kuz'min, V.A. Kazantsev, S.K. Sidorov and V.N. Kalinin, Phys. Met. Metallogr. (USSR) 40 (1975) 174.
- [3] S.B. Roy, A.K. Majumdar, N.C. Mishra, A.K. Raychaudhury and R. Srinivasan, Phys. Rev. B 31 (1985) 7458.
- [4] T.K. Nath and A.K. Majumdar, J. Appl. Phys. 70 (1991) 5828.
- [5] J.A. Ewing, Philos. Trans. (London) 176 (1885) 523.
- [6] G. Richter, Ann. Phys. (Leipzig) 29 (1937) 605.
- [7] R. Street and J.C. Woolley, Proc. Phys. Soc. (London) A 62 (1949) 562; B 63 (1950) 509; B 69 (1956) 1189; R. Street, J.C. Woolley and P.B. Smith, Proc. Phys. Soc. B 65 (1952) 679.
- [8] L. Néel, Ann. Univ. Grenoble 22 (1946) 299.
- [9] K.L. Ngai, Comments Solid State Phys. 9 (1979) 127; 9 (1980) 141.
- [10] G. Williams and D.C. Watts, Trans. Faraday Soc. 66 (1970) 80.
- [11] A.K. Jonscher, Nature 267 (1977) 673.
- [12] M.H. Cohen and G.S. Grest, Phys. Rev. B 24 (1981) 4091.
- [13] R.V. Chamberlin, G. Mozurkenich and R. Orbach, Phys. Rev. Lett. 52 (1984) 867.
- [14] R. Hoogerbeets, Wei-Li Luo and R. Orbach, Phys. Rev. Lett. 55 (1985) 111.
- [15] F. Mezei and A.P. Murani, J. Magn. Magn. Mater. 14 (1979) 211.
- [16] R.V. Chamberlin, J. Appl. Phys. 57 (1985) 3377.

- [17] P. Nordblad, P. Svedlindh, L. Lundgren and L. Sandlund, *Phys. Rev. B* 33 (1986) 645.
- [18] R.G. Palmer, D.L. Stein, E. Abrahams and P.W. Anderson, *Phys. Rev. Lett.* 53 (1984) 958.
- [19] M.F. Schlesinger and E.W. Montroll, *Proc. Nat. Acad. Sci. USA* 81 (1984) 1280.
- [20] J. Hammann, M. Ocio and E. Vincent, in *Relaxation in Complex Systems and Related Topics*, eds. I.A. Campbell and C. Giovannella (Plenum, New York, 1990) p. 11.
- [21] L. Lundgren, P. Nordblad and P. Svedlindh, *Phys. Rev. B* 34 (1986) 8164.
- [22] R. Tournier and Y. Ishikawa, *Phys. Lett.* 11 (1964) 280.
- [23] S. Oseroff, M. Mesa, M. Tovar and R. Arce, *J. Appl. Phys.* 53 (1982) 2208; C.N. Guy, *J. Phys. F* 8 (1978) 1309.
- [24] A.P. Murani, *J. Phys. F* 15 (1985) 417.
- [25] N. Bontemps and R. Orbach, *Phys. Rev. B* 37 (1988) 4708.
- [26] G. Parisi, *Phys. Lett. A* 73 (1979) 203; *Phys. Rev. Lett.* 43 (1979) 1574; *Phys. Rev. Lett.* 50 (1983) 1946; M. Mezard, G. Parisi, N. Sourlas, G. Toulouse and M.A. Virasoro, *Phys. Lett.* 52 (1984) 1156; M. Mezard, G. Parisi and M.A. Virasoro, *Spin Glass Theory and Beyond*, in *Lecture Notes in Physics*, Vol. 9 (World Scientific, Singapore, 1987).
- [27] S. Kirkpatrick and D. Sherrington, *Phys. Rev. B* 17 (1978) 4348.
- [28] P. Sibani, *Phys. Rev. B* 35 (1987) 8572; P. Sibani and K.H. Hoffmann, *Phys. Rev. Lett.* 63 (1989) 2853.
- [29] D.A. Huse and D.S. Fisher, *Phys. Rev. B* 35 (1987) 6841; *B* 38 (1988) 373, 386; *Phys. Rev. Lett.* 56 (1986) 1601; A.J. Bray and M. Moore, *Phys. Rev. Lett.* 58 (1987) 57.
- [30] G. Koper and H. Hilhorst, *J. Phys. (Paris)* 49 (1988) 429.
- [31] F. Iefloch, J. Hammann, M. Ocio and E. Vincent, *Europhys. Lett.* 18(7) (1992) 647.
- [32] A.T. Ogileski, *Phys. Rev. B* 32 (1985) 7384.
- [33] K. Gunnarsson, P. Svedlindh, P. Norblad and L. Lundgren, *Phys. Rev. Lett.* 61 (1988) 754.
- [34] M. Ocio, M. Alba and J. Hammann, *J. Phys. Lett. (Paris)* 46 (1985) L1101.
- [35] M. Alba, M. Ocio and J. Hammann, *Europhys. Lett.* 2(1) (1986) 45.
- [36] H. Sompolinsky and A. Zippelius, *Phys. Rev. Lett.* 47 (1981) 359.
- [37] R.V. Chamberlin and D.N. Haines, *Phys. Rev. Lett.* 65 (1990) 2197.
- [38] R.J. Borg and T.A. Kitchens, *J. Appl. Chem. Solids* 34 (1973) 1323.
- [39] J.D. Gunton, M. Sam Miguel and P.S. Sahui, in *Phase Transitions and Critical Phenomenon*, eds. C. Domb and J.L. Lebowitz (Academic Press, New York, 1983) Vol. 8.
- [40] P.C. Hohenberg and B.I. Halperin, *Rev. Mod. Phys.* 49 (1977) 435.
- [41] H. Ikeda and K. Kikuta, *J. Phys. C*, 17 (1984) 1221.
- [42] M. Gabay and G. Toulouse, *Phys. Rev. Lett.* 47 (1981) 201.
- [43] K. Binder and A.P. Young, *Rev. Mod. Phys.* 58 (1986) 801.
- [44] R.V. Chamberlin, *Phys. Rev. B* 30 (1984) 5393.
- [45] D. Chu, G.G. Kenning and R. Orbach, *Phys. Rev. Lett.* 72 (1994) 3270.
- [46] D. Chu, G.G. Kenning and R. Orbach, *Philos. Mag. B* 71 (1995) 479.
- [47] P. Mitchler, R.M. Roshko and W. Ruan, *J. Phys. I France* 2 (1992) 2299; D. Li, R.M. Roshko and G. Yang, *Phys. Rev. B* 49 (1994) 9601.
- [48] R.V. Chamberlin and F. Holtzberg, *Phys. Rev. Lett.* 67 (1991) 1606.
- [49] D. Stauffer, A. Caniglio and M. Adam, *Adv. Polim. Sci.* 44 (1982) 103.
- [50] T.K. Nath, N. Sudhakar, A.K. Majumdar and E.J. McNiff, Jr., *Annual Report, Francis Bitter National Magnet Laboratory, Massachusetts Institute of Technology* (1991–1992) p. 77.
- [51] T. Taniguchi, Y. Miyako and J.L. Tholence, *J. Phys. Soc. Jpn.* 54 (1985) 220.
- [52] M. Suzuki, *Prog. Theor. Phys.* 58 (1977) 1151.
- [53] S.F. Edwards and P.W. Anderson, *J. Phys. F* 5 (1975) 965.
- [54] G. Sinha and A.K. Majumdar (communicated).